


# Mass production of industrial tunnel oxide passivated contacts (i-TOPCon) silicon solar cells with average efficiency over 23% and modules over 345 W

Yifeng Chen<sup>1</sup>  | Daming Chen<sup>1</sup> | Chengfa Liu<sup>1</sup> | Zigang Wang<sup>1</sup> | Yang Zou<sup>1</sup> | Yu He<sup>1</sup> | Yao Wang<sup>1</sup> | Ling Yuan<sup>1</sup> | Jian Gong<sup>1</sup> | Wenjie Lin<sup>1,2</sup> | Xueling Zhang<sup>1</sup> | Yang Yang<sup>1</sup> | Hui Shen<sup>2</sup> | Zhiqiang Feng<sup>1</sup> | Pietro P. Altermatt<sup>1</sup> | Pierre J. Verlinden<sup>1,2,3</sup>

<sup>1</sup>State Key Lab of Photovoltaic Science and Technology, Trina Solar, Changzhou 213031, China

<sup>2</sup>Institute for Solar Energy Systems, Sun Yat-Sen University, Guangzhou 510006, China

<sup>3</sup>AMROCK Pty Ltd, McLaren Vale, South Australia 5171, Australia

## Correspondence

Yifeng Chen and Daming Chen, State Key Lab of Photovoltaic Science and Technology, Trina Solar, Changzhou 213031, China.

Email: yifeng.chen01@trinasolar.com; daming.chen01@trinasolar.com

## Funding information

Technology Top Runner Program of China; National 10,000 Talents Program in China

## Abstract

We present an industrial tunnel oxide passivated contacts (i-TOPCon) bifacial crystalline silicon (c-Si) solar cell based on large-area *n*-type substrate. The interfacial thin SiO<sub>2</sub> is thermally growth and in situ capped by an intrinsic poly-Si layer deposited by low-pressure chemical vapor deposition (LPCVD). The intrinsic poly-Si layer is doped in an industrial POCl<sub>3</sub> diffusion furnace to form the *n*<sup>+</sup> poly-Si at the rear, which shows an excellent surface passivation characteristics with  $J_0 = 2.6 \text{ fA/cm}^2$  when passivated by a SiN<sub>x</sub>:H layer deposited by plasma-enhanced chemical vapor deposition (PECVD). With an industrial fabrication process, the cells are manufactured with screen-printed front and rear metallization, using large-area 6-in. *n*-type Czochralski (Cz) Si wafers. We demonstrate an average front-side efficiency greater than 23% and an open-circuit voltage  $V_{oc}$  greater than 700 mV. These results are based on more than 20 000 pieces of cells from mass production on a single day, in an old conventional multicrystalline silicon (mc-Si) Al-back surface field (BSF) cell workshop, which has been upgraded to i-TOPCon process. The best cell efficiency reaches 23.57%, as independently confirmed by Fraunhofer CalLab. A median module power greater than 345 W and a best module power greater than 355 W are demonstrated with double-glass bifacial i-TOPCon modules consisting of 120 pieces of half-cut 161.7 mm pseudosquare i-TOPCon cells with nine busbars.

## KEYWORDS

bifacial, industrial, *n*-type, passivated contacts, screen printing

## 1 | INTRODUCTION

The efficiency of silicon wafer-based commercial photovoltaic (PV) modules has been rapidly improving over the past decades with an average annual growth of 0.3%<sub>abs</sub> to 0.4%<sub>abs</sub>.<sup>1</sup> These improvements have been supported not only by industrial research and development (R&D) but remarkably also by public research laboratories and institutes. For example, the efficiency of today's mass-produced

monocrystalline cells with a full-area Al-back surface field (BSF) reaches 20.5% to 21.0% in air, partly due to improvements and optimization in commercial fabrication, but mostly due to long-term R&Ds such as firing-through processes, hydrogenation via SiN<sub>x</sub>:H, and reduction of inactive phosphorous in diffusions. Regarding the production of passivated emitter and rear cell (PERC) cells that was first introduced in the 1980s,<sup>2</sup> many manufacturers are reaching an average cell efficiency in air of 22.3%,<sup>3</sup> thanks to the selective emitter, the rear

passivation, and the optimized rear laser opening. All of these high-efficiency processes, which were initiated by public R&D institutions, contributed significantly to the increase of the efficiency of industrial large-area PERC cells, approaching the “dedicated-area” efficiency record demonstrated in laboratory on small-area cells. As most parts of front and rear sides of the industrial PERC cells are well passivated,<sup>4</sup> further improvements now focus on reducing the recombination underneath the metal contacts and recombination in the bulk.<sup>5</sup>

Presently, strong stimulation for passivating contacts comes from public institutions, as they have the necessary analytical tools available and are free to try out new structures and materials than the industrial R&D laboratories. Excellent balance has been achieved among the two key properties of passivating contacts: recombination and contact resistivity.<sup>6</sup> Although various structures and materials have been proposed,<sup>7</sup> the industry has so far adopted mainly two different approaches: a low-temperature passivated contact using intrinsic a-Si/doped a-Si heterojunction stacks and a high-temperature passivated contact using tunnel SiO<sub>x</sub>/doped poly-Si stacks. The well-known heterojunction stack has been applied in industrial mass production since 1990, the “heterojunction with intrinsic thin-layer” (HIT)<sup>8</sup> cell technology, with the efficiency of the best champion cell being greater than 25%,<sup>9,10</sup> and presently reaching median efficiencies of 23.3% in industrial production (Jun Zhao, Meyer Burger, Germany, private communication by email in January 2019). The best cell efficiency, reached in the laboratory with such heterojunctions, presently is 26.7%<sup>11</sup> with a rear-contacted geometry.

The tunnel SiO<sub>x</sub>/doped poly-Si was investigated in bipolar transistor technology in the 1970s.<sup>12–17</sup> The pioneer applications<sup>18–22</sup> in PV started around 1980 and passivating contacts were commercialized in 2009 by SunPower Corp.<sup>23</sup> However, very recently, the tunnel SiO<sub>x</sub>/doped poly-Si attracted wide interest and attention, after Feldmann et al reported over 23% in efficiency on small-area *n*-type substrate,<sup>24</sup> with the tunnel oxide passivated contacts (TOPCon) cell structure. The best monofacial cell efficiency of 25.8%<sup>25</sup> with front and rear contacts is currently held by Fraunhofer ISE,<sup>26</sup> using SiO<sub>x</sub>/poly-Si stacks. The champion cell from Glunz and Feldmann<sup>25</sup> has a selective boron emitter, and a tunnel SiO<sub>x</sub>/poly-Si (*n*<sup>+</sup>) stacks on the rear side, using Ti/Pd/Ag plating and full-area Ag for front and rear metallization, respectively. With a rear-contacted geometry, a 26.1% efficiency was reported with thin SiO<sub>x</sub>/doped poly-Si passivation by ISFH.<sup>27</sup>

The success of development of TOPCon cell in the laboratory attracted the attention and interest of the PV industry. Inspired by the work of these institutes, we have developed an industrial tunnel oxide passivated contacts (i-TOPCon) cell since 2015. Comparing with the TOPCon cell developed by Fraunhofer ISE,<sup>25</sup> the biggest difference is that we introduce a bifacial cell structure and a double-side screen printing metallization into the i-TOPCon cell. In this paper, we report a median front-side efficiency greater than 23% for *n*-type i-TOPCon bifacial crystalline silicon (c-Si) solar cells in mass production. To the best of our knowledge, this is the first report of 23% of bifacial TOPCon cells in mass production. The best efficiency reaches 23.57% that was independently certificated by the Fraunhofer CalLab.

The front power output were demonstrated to be greater than 345 W<sub>p</sub> in double-glass bifacial i-TOPCon modules based on 60 pieces of 161.7 mm quasi-square i-TOPCon cells with median efficiency of 23%.

## 2 | NEW WORKSHOP DESIGN

We started the study of thin SiO<sub>x</sub>/poly-Si (*n*<sup>+</sup>) passivation in 2015 and developed an industrial cell structure and process flow of i-TOPCon cell in the State Key Lab of Photovoltaic Science and Technology (SKL) in Trina Solar. In 2018, we demonstrated a champion efficiency of 23.1%, which was independently confirmed by JET Japan,<sup>28</sup> and started to transfer the technology from the SKL to a manufacturing workshop in Trina Changzhou. The workshop is an 8-year-old cell factory with full-scale production of conventional multicrystalline silicon (mc-Si) cell with full-area Al-BSF. It was even more challenging to design the new workshop for the i-TOPCon technology, by keeping (a) as many as possible tools from the previous mc-Si lines and (b) these tools at the same positions without moving, to extend the lifetime of these tools and the facility, and to minimize the capital investment. After careful considerations, we only removed the old acid texture tools for mc-Si cells. To save space, we custom designed an industrial alkaline texturing wet bench that has a throughput of 8000 pieces per hour. We upgraded the previous Tempres POC<sub>3</sub> diffusion furnaces into boron diffusion tools. We kept the previous remote plasma-enhanced chemical vapor deposition (PECVD) SiN<sub>x</sub>:H tools from Roth&Rau and the previous screen printers from Baccini. We also introduced new tools, including low-pressure chemical vapor deposition (LPCVD) and new surface passivation tools. The cell flash testers were upgraded since the i-TOPCon cells have much higher capacitance compared with normal mc-Si BSF cells. The upgrading of the workshop to i-TOPCon started from Q3 2018, and we started production in late 2018.

## 3 | EXPERIMENTAL DETAILS

The i-TOPCon solar cell structure is illustrated in Figure 1 with a fabrication process flow shown in Figure 2. The cell is based on M4 (161.7-mm quasi-square) large-area Czochralski (Cz) *n*-type silicon wafers with resistivity of 0.2 to 2 Ω·cm. The wafers are double-side textured in alkaline solutions to form pyramid structures. After the alkaline texturing, the wafers are put into the boron diffusion furnace to form a homogeneous *p*<sup>+</sup> emitter. The rear *p*<sup>+</sup> region is removed using a single-side inline wet bench. The thermal oxidation and the in situ intrinsic polysilicon (i-poly) with a thickness of 200 TO 300 nm are grown in an industrial LPCVD tool. A POC<sub>3</sub> diffusion is carried out to dope the intrinsic poly into *n*<sup>+</sup>. As there is no inline tool available, we do not have the ability to measure the thickness of the thin oxide, and we can only approximately measure the thickness of polysilicon. There layers are therefore fine-tuned in an empirical way. A single-side etching (SSE) is used to remove the wrap around *n*<sup>+</sup> polyarea without damaging the boron emitter. After wet chemical

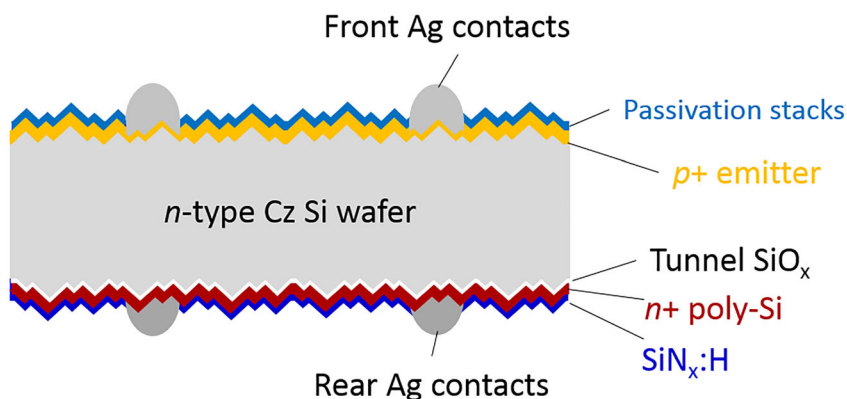


**FIGURE 1** Cross section schematic of industrial tunnel oxide passivated contacts (i-TOPCon) bifacial cell based on *n*-type Czochralski (Cz) silicon substrate with front and rear screen-printed contacts [Colour figure can be viewed at [wileyonlinelibrary.com](http://wileyonlinelibrary.com)]

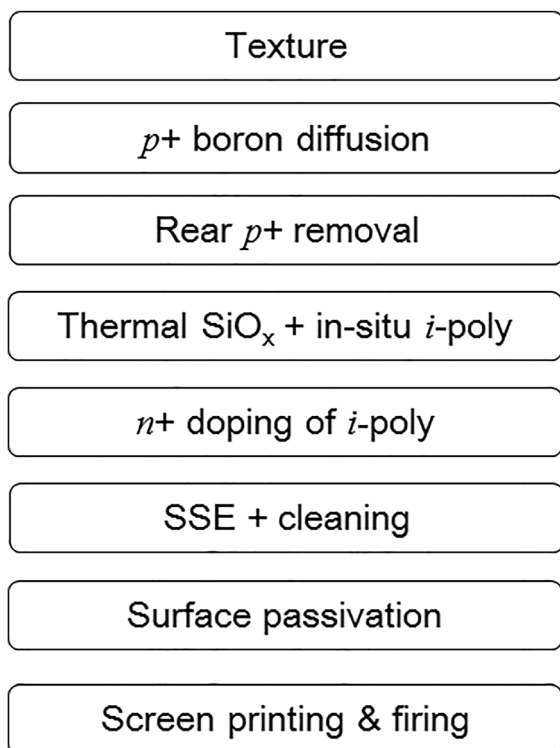


**FIGURE 2** Fabrication process of the industrial tunnel oxide passivated contacts (i-TOPCon) cells with structure illustrated in Figure 1 used in an industrial mass production

cleaning, the front boron emitter of the cell is well passivated by a thin film stack, while the rear side poly-Si ( $n^+$ ) is passivated by  $\text{SiN}_x\text{:H}$  deposited by PECVD. Finally, the cells are screen printed with an “H-pattern” metal contact pattern on both sides. The front-side metalization is done with dual print, meaning the fingers are screen printed with firing-through paste, while the busbars with nonfiring through paste. The cells are fired at a peak temperature of around  $760^\circ\text{C}$  to  $780^\circ\text{C}$ .

To evaluate the passivation effect of the tunnel oxide and poly-Si ( $n^+$ ) stacks, we fabricated symmetrical lifetime samples for lifetime and  $J_0$  measurements. These samples are fabricated on high-lifetime *p*-type Cz commercial wafers with resistivities over  $20\ \Omega\cdot\text{cm}$ . The

wafers are double-side wet-chemically polished using 10% KOH solution for 5 minutes and cleaned from KOH residues by a standard RCA process. After the polishing, the samples were put into the industrial LPCVD machine for thermal oxidation and in situ polydeposition, followed by a  $\text{POCl}_3$  diffusion in the tube furnace, using the same recipes as for the real production cells. Each sample occupies a simple slot, to form the poly-Si ( $n^+$ )/ $\text{SiO}_x$ /Si ( $n$ )/ $\text{SiO}_x$ /poly-Si ( $n^+$ ) symmetrical structure. The samples are double side passivated by  $\text{SiN}_x\text{:H}$  by PECVD. Finally, the samples were processed with an industrial firing process with a peak temperature of about  $760^\circ\text{C}$  to  $780^\circ\text{C}$ .

## 4 | RESULTS AND DISCUSSION

### 4.1 | Thin $\text{SiO}_x$ /poly-Si ( $n^+$ ) passivation

All the lifetime samples were measured using the transient mode of the photo-conductance decay (PCD) method<sup>29</sup> with a WCT-120 from Sinton Instrument. When each sample is injected via light, the excess carrier density  $\Delta n_{\text{mid}}$  at half-depth of the sample is always higher than the  $\Delta n_{\text{surf}}$  in the regions at the front and rear surfaces, despite the small amount of recombination of such stacks. As the gap between  $\Delta n_{\text{mid}}$  and  $\Delta n_{\text{surf}}$  is injection dependent, we plot the saturation current density  $J_0$  as a function of the injection carrier density and take the largest value in high injection to avoid underestimation of  $J_0$ .<sup>30</sup> The single-side  $J_0$  for thin  $\text{SiO}_x$ /poly-Si ( $n^+$ ) passivated  $\text{SiN}_x\text{:H}$  is illustrated in Figure 3. Very good surface passivation can be achieved with a  $J_0$  down to  $2.6\ \text{fA}/\text{cm}^2$ , using an intrinsic carrier density of  $8.6 \times 10^9\ \text{cm}^{-3}$  in the data evaluation. This value of  $J_0$  agrees well with the result of  $2.7\ \text{fA}/\text{cm}^2$  in previous publications,<sup>6,31</sup> only a little bit higher than the  $J_0$  of a-Si (*i*)/a-Si ( $n^+$ ) stacks, which has been demonstrated to be as low as  $2\ \text{fA}/\text{cm}^2$ .<sup>32</sup> This result demonstrates the excellent passivation of  $\text{SiO}_x$ /poly-Si ( $n^+$ ) stacks in a production LPCVD tool and with an external diffusion furnace.

### 4.2 | Cells results

The factory for i-TOPCon cells is fully running. In 4 March 2019, we took the data of 1 day's production from one screen printing line,

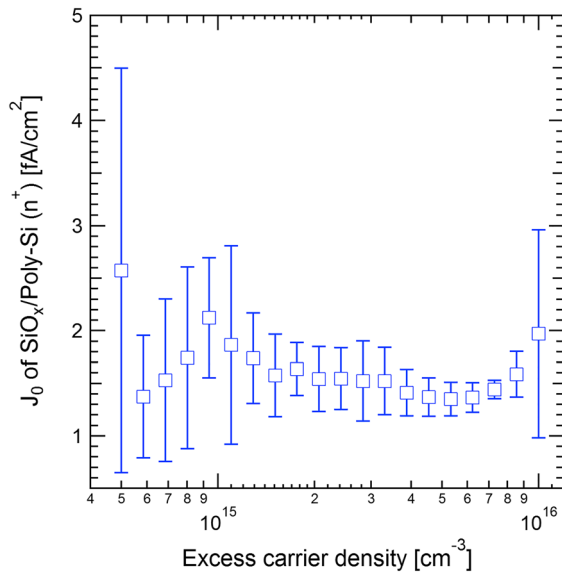


**FIGURE 3** Single-side  $J_0$  of thin oxide  $\text{SiO}_x/\text{poly-Si}$  ( $n^+$ ) as a function of excess carrier density that was passivated by  $\text{SiN}_x:\text{H}$  with plasma-enhanced chemical vapor deposition (PECVD). The error bar represents the results of three samples and measurements of 5 points in each sample [Colour figure can be viewed at [wileyonlinelibrary.com](#)]

which corresponds to more than 20 000 pieces of cells. The cells were measured via an inline FCT 750 I-V tester from Sinton Instrument, using a reference cell that was independently calibrated in JET in Japan. As the cells are bifacial, the rear side of the cells is covered by a black sheet with an average reflectivity of less than 3%.

As shown in Table 1, the median efficiency reaches 23.0% with a median  $V_{oc}$  of 701.5 mV. To the best of our knowledge, this is the first report of 23% total-area efficiency of i-TOPCon cells in industrial mass production. The distribution of efficiency and  $V_{oc}$  is plotted in Figure 4

**TABLE 1** Summary of the I-V results for 20 000 pieces of i-TOPCon cells when the front side is illuminated

	$J_{sc}$ , mA/cm <sup>2</sup>	$V_{oc}$ , mV	FF, %	Efficiency, %
Median	39.84	701.5	82.2	23.0

Abbreviation: i-TOPCon, industrial tunnel oxide passivated contacts.

. Only less than 1% of the cells have efficiency less than 22.3% and  $V_{oc}$  less than 690 mV, while 75% of the cells have an efficiency greater than 22.85% and a  $V_{oc}$  greater than 699 mV. The efficiency distribution is highly skewed, and the cells in the largest bin have an efficiency of 23.05% and a  $V_{oc}$  of 703 mV. This indicates that the median efficiency will be soon improved by reducing the parameter variability in the cell process. The best laboratory champion cell with an improved boron emitter was independently measured by Fraunhofer CalLab with front-side efficiency of 23.57% and  $V_{oc}$  of 716.7 mV and bifaciality of 80.5% (efficiency bifaciality) or 81.2% ( $J_{sc}$  bifaciality), shown in Table 2. The  $J_{0,e}$  of the passivated boron emitter can be reduced from 25 to 30 fA/cm<sup>2</sup> (baseline emitter) down to 15 to 18 fA/cm<sup>2</sup> (improved emitter). This indicates the further efficiency roadmap for i-TOPCon cells towards 23.5% efficiency and higher, by reducing the recombination of the boron emitter and the contact area.

To further understand the efficiency improvement of i-TOPCon cells, we calculated the total  $J_0$  of a cell by using the one-diode equation:

$$J_{0,\text{total}} = \frac{J_{sc}}{\exp\left(\frac{qV_{oc}}{nk_B T}\right) - 1}, \quad (1)$$

where  $J_{0,\text{total}}$  is the total  $J_0$  of the i-TOPCon cell,  $J_{sc}$  is the short circuit current density,  $q$  is the elementary charge,  $V_{oc}$  is the open-circuit voltage,  $n$  is the ideality factor,  $k_B$  is the Boltzmann constant, and  $T$  is the absolute temperature. In the following calculation, we set  $n = 1$ . Figure 5 depicts cell efficiency (front side, blue dots) as a function of  $J_{0,\text{total}}$ , compared with manufactured PERC cells (red dots) with median efficiency of 22.25%. By fixing  $J_{sc} = 39.85 \text{ mA/cm}^2$ , we also plot the yellow dashed curve. The PERC efficiencies are higher than the yellow curve because the  $J_{sc}$  of PERC is higher than of i-TOPCon, due to the

**TABLE 2** Best champion i-TOPCon cell with more optimized boron emitter and  $\text{SiO}_x/\text{SiN}_x:\text{H}$  front antireflection coating independently confirmed by Fraunhofer CalLab

	$J_{sc}$ , mA/cm <sup>2</sup>	$V_{oc}$ , mV	FF, %	Efficiency, %	Bifaciality, %
Front side	40.14	716.7	82.0	23.57	80.5 (eff.)
Rear side	32.59	710.8	81.9	18.98	81.2 ( $J_{sc}$ )

Abbreviation: i-TOPCon, industrial tunnel oxide passivated contacts.

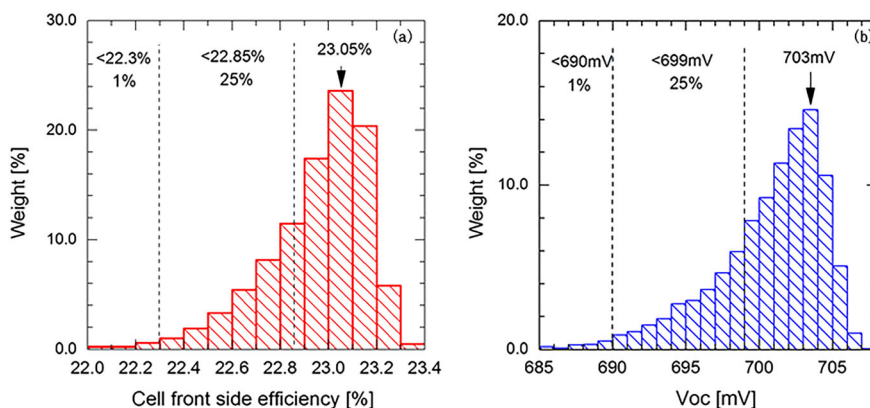


**FIGURE 4** Efficiency of front side, and  $V_{oc}$  distribution for over 20 000 pieces of cells produced in the production line for a single day [Colour figure can be viewed at [wileyonlinelibrary.com](#)]



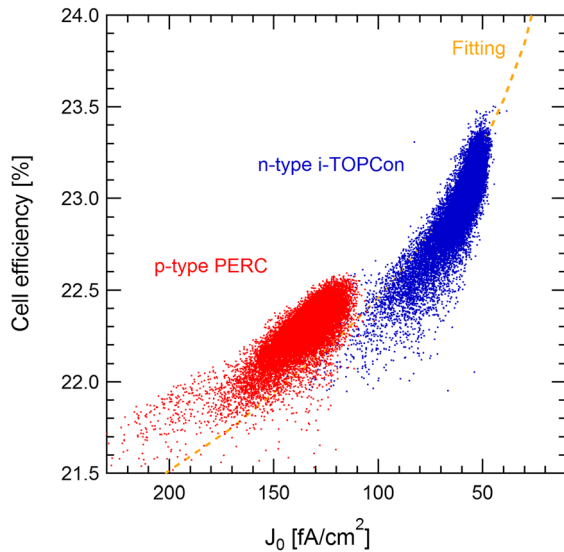


**FIGURE 5** Cell efficiency of industrial tunnel oxide passivated contacts (i-TOPCon) cell (blue points) and PERC cell (red points) as a function of calculated  $J_{0,\text{total}}$  [Colour figure can be viewed at [wileyonlinelibrary.com](http://wileyonlinelibrary.com)]

strong parasitic absorption of the rear poly-Si ( $n^+$ ) layers in i-TOPCon cells. The key improvement of i-TOPCon is the reduction of the total carrier recombination with typical  $J_{0,\text{total}}$  going down to 60 fA/cm<sup>2</sup> and  $V_{oc}$  going above 700 mV, while  $J_0$  of industrial PERC cells is in the range of 100 to 150 fA/cm<sup>2</sup>.

The advantage of reducing the  $J_{0,\text{total}}$  is for improving not only the  $V_{oc}$  but also the FF. We plot the fill factor  $FF_0$  for the ideality factor  $n = 1$ , as a function of  $V_{oc}$ , shown by the dashed curve in Figure 6, using the equation from Green<sup>33</sup>:

$$FF_0 = \frac{V_{oc} - \ln(V_{oc} + 0.72)}{V_{oc} + 1}, \quad (2)$$

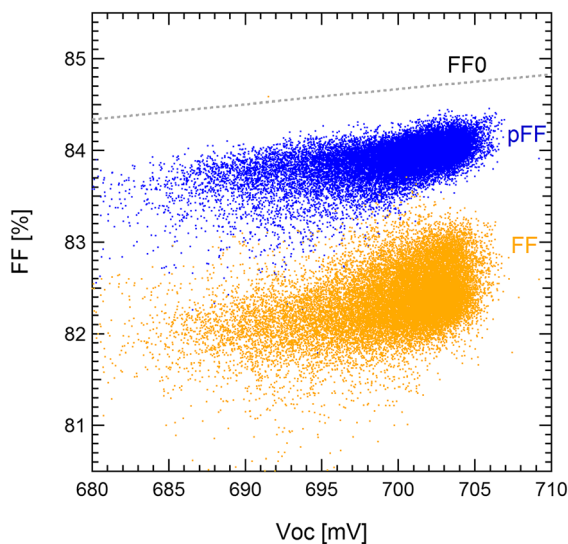


**FIGURE 6**  $FF_0$ ,  $pFF$ , and  $FF$  of industrial tunnel oxide passivated contacts (i-TOPCon) cells as a function of  $V_{oc}$  [Colour figure can be viewed at [wileyonlinelibrary.com](http://wileyonlinelibrary.com)]

where  $v_{oc} = V_{oc}/nk_B T$ ,  $V_{oc}$  is the open-circuit voltage,  $k_B$  is the Boltzmann constant, and  $T$  is the temperature. With the Sinton FCT-750, we also measure the pseudofill factor  $pFF$  for each cell from the suns- $V_{oc}$  curve, as indicated by blue dots in Figure 6. Both  $FF_0$  and  $pFF$  increase with  $V_{oc}$ . The difference between  $FF_0$  and  $pFF$  indicates that the ideality factor is not exactly equal to 1 and that the effective recombination lifetime is varying with carrier injection level, ie, varies with the cell voltage. By applying the multibusbar technology, we aim to minimize the series resistance  $R_s$ , which typically introduces about 1.2% to 1.5% absolute fill factor loss from  $pFF$ .

To optimize the wafer resistivity for i-TOPCon cells, we extensively use the Sinton Instruments FCT-750 flash tester for this purpose. The graph in Figure 7 shows the measured effective carrier lifetime of i-TOPCon cells working at the maximum power point, with respect to the measured doping concentration of the bulk material, taken from a typical commercial Cz  $n$ -type ingot with wafer resistivity varying from 0.2 to 2  $\Omega\cdot\text{cm}$ . The effective carrier lifetime shows very little dependence on the wafer doping, which is a good indication that cell efficiency is not so strongly correlated to the wafer resistivity (apart from the built-in voltage across the pn-junction). It also means that the specification for wafer resistivity can be very wide. The wafer resistivity distribution is normally wider in  $n$ -type phosphorus-doped Cz ingots than in a boron-doped  $p$ -type ingots. This is because the segregation coefficient of phosphorus is smaller than for boron. This observation of Figure 7 that an almost constant carrier lifetime versus doping level allows the PV industry to fully utilize the whole  $n$ -type Cz ingot and to expect that the cost of the  $n$ -type wafers can be reduced. The intrinsic lifetime (ie, Auger and radiative recombination) at the injection level of  $1 \times 10^{15} \text{ cm}^{-3}$  as a function of base doping is also plotted in Figure 7 for comparison (dotted line), by using the latest

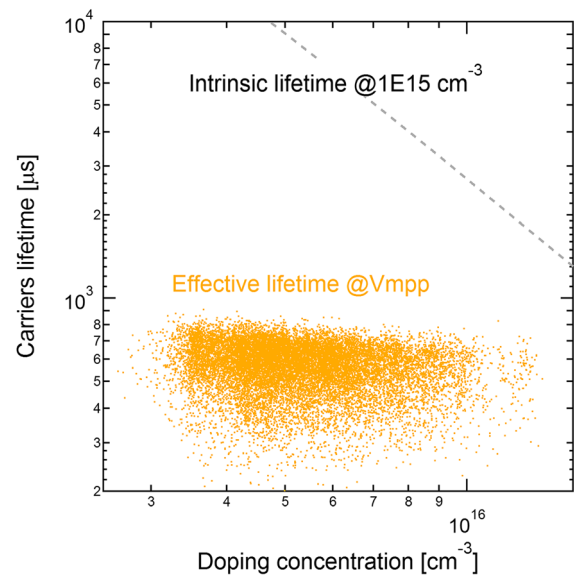


**FIGURE 7** Effective lifetime at  $V_{mpp}$ , derived with the inline FCT-750 cell tester, compared with the intrinsic lifetime at  $1 \times 10^{15} \text{ cm}^{-3}$ , as a function of doping concentration of the Czochralski (Cz)  $n$ -type wafer of mass-produced industrial tunnel oxide passivated contacts (i-TOPCon) cells [Colour figure can be viewed at [wileyonlinelibrary.com](http://wileyonlinelibrary.com)]

update<sup>34</sup> of the parametrization of Auger recombination by Richter et al.<sup>35</sup> Note that the injection level for i-TOPCon cells at  $V_{mpp}$  is not fixed but varies from  $1.6 \times 10^{15} \text{ cm}^{-3}$  to  $2.4 \times 10^{15} \text{ cm}^{-3}$ , and the intrinsic lifetime at injection of  $1 \times 10^{15} \text{ cm}^{-3}$  can only be used here as a reference. A strong decay of intrinsic lifetime above a base doping of  $1 \times 10^{16} \text{ cm}^{-3}$  is apparent due to Auger recombination. The difference of the intrinsic to the effective lifetime data indicates that the recombination at the front and back region dominate in our i-TOPCon cells. The efficiency could be further improved by suppressing the recombination at the front and the rear, without changing the bulk material.

As we optimize the i-TOPCon cell structure and cell or process parameters, it is important to focus our work more on voltage improvements than current improvements. Many years ago, when the quality of silicon wafers was not as good as it is nowadays, using low-resistivity wafers was the mean to maintain a high open-circuit voltage. With the quality of wafers improving and the bulk carrier lifetime increasing, we are able to use less doped silicon wafers and higher resistivity. This study is important since the cost of *n*-type silicon wafers is highly dependent on the specification for the range of resistivity and minimum carrier lifetime. The product of the bulk carrier lifetime and the substrate doping density is a good indication of the " $V_{oc}$  capability" of the solar cell. Unfortunately, we do not have access to the real bulk carrier lifetime but the effective carrier lifetime, which includes the surface, contact, and emitter recombination. The cell efficiency and  $V_{oc}$  as a function of the product of effective lifetime at  $V_{mpp}$  and substrate doping density ( $\tau_{eff} \times N_A$ ) is plotted in Figure 8. From the data in Figure 8, for wafers with low carrier lifetime (low-efficiency cells), the cell efficiency is slightly improved by increasing the doping density of the substrate. However, for wafers with high carrier lifetime (highest efficiency cells), the cell efficiency decreases slightly if the doping density increases due to a reduction of  $I_{sc}$ . In this

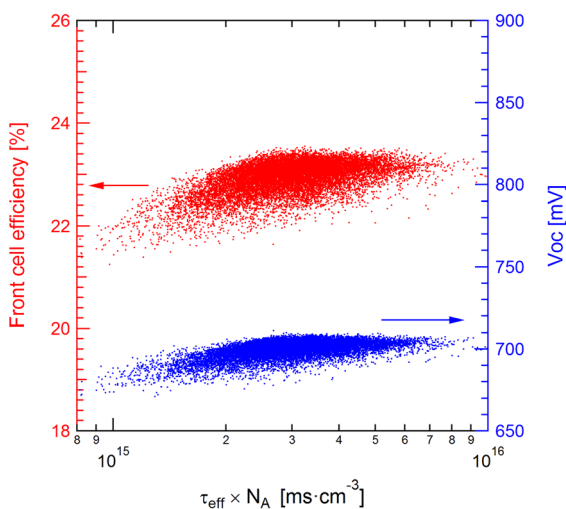


**FIGURE 8** Cell efficiency (front side, red) in left axis and  $V_{oc}$  (blue) in right axis as a function of the product of measured effective carrier lifetime at  $V_{mpp}$  and doping concentration for *n*-type industrial tunnel oxide passivated contacts (i-TOPCon) cells [Colour figure can be viewed at [wileyonlinelibrary.com](http://wileyonlinelibrary.com)]

**TABLE 3** I-V parameters of i-TOPCon modules with illumination from front side

	$V_{oc}$ , V	$I_{sc}$ , A	FF, %	$P_{max}$ , W
Median	41.6	10.4	80.1	346.6
Best	42.2	10.5	80.4	356.2

Abbreviation: i-TOPCon, industrial tunnel oxide passivated contacts.

experiment and with this large batch of cells, the highest efficiency is obtained for an optimum lifetime-doping product of about  $2.5 \times 10^{15} \text{ ms/cm}^3$ .

### 4.3 | Manufacture of i-TOPCon modules

The industrial i-TOPCon module consists of 60 pieces of i-TOPCon cells ( $161.7 \text{ mm} \times 161.7 \text{ mm}$  pseudosquare, with a total area of  $258.25 \text{ cm}^2$ ). The cells are half-cut by laser, and soldered via nine copper wires coated with Sn and Pb. The cells are double-side laminated between two 2.0-mm tempered glass panels to form bifacial modules. In the gap between cells, a layer of reflective powder, which contains calcium carbonate, is screen printed on the surface of the rear glass, while the area below the cells is transparent. This enables a selective reflection of light falling between cells to enhance the light recycling at the module level while maintaining a bifacial structure. The modules are measured by an inline module tester, with a reference module of the same cell technology calibrated in TÜV Rheinland in Shanghai. During the measurement, the rear side of the module is covered with a black sheet.

The manufacturing of i-TOPCon modules started in January 2019. Table 3 shows the median and best performance of i-TOPCon modules that were produced in March 2019. Over 345  $W_p$  median power was achieved with a champion module power greater than 355  $W_p$ . The power bifaciality of the i-TOPCon modules ranges from 75% to 80%. Therefore, a total power output of the best i-TOPCon 60-cell module may rise to 397.6 W, with an additional 0.15 sun illumination from rear side.<sup>36</sup> By using the *n*-type wafer as substrate to avoid the light-induced degradation (LID) due to B-O complex, the LID for i-TOPCon is less than 1%. By encapsulated with double glass, it is hard for moisture to penetrate into the module. This enables i-TOPCon modules to have better reliability.

## 5 | CONCLUSIONS

The ultrathin tunnel  $\text{SiO}_x/\text{poly-Si}(n^+)$  passivating contacts are becoming a key process for mass-produced cells to further improve efficiency above 23%. In this paper, we propose an i-TOPCon bifacial solar cell based on screen printing technology. The i-TOPCon cells were fabricated via a lean process flow that is feasible for mass production, with the ultrathin tunnel oxide and intrinsic polysilicon in situ growth in an industrial LPCVD tool. Excellent surface passivation with a recombination parameter  $J_0$  of  $2.6 \text{ fA/cm}^2$  is demonstrated with thin  $\text{SiO}_x/\text{poly-Si}(n^+)/\text{SiN}_x/\text{H}$  stacks. The i-TOPCon technology has been successfully

demonstrated in a full-scale mass production. Median efficiency over 23% (front side) is reported for the first time with  $V_{oc}$  greater than 700 mV. A champion i-TOPCon cell with efficiency of 23.57% and  $V_{oc}$  of 716.7 mV was independently confirmed by Fraunhofer CalLab. The key to high-efficiency i-TOPCon cell is the relative low carrier recombination within the whole cell, supported by a typical  $J_{0,total}$  approximately 60 fA/cm<sup>2</sup>. Median module power over 345 W and a best module power over 355 W are demonstrated with a double-glass bifacial structure consisting of 120 pieces of half-cut 161.7 mm pseudosquare i-TOPCon cells with nine busbars. The successful transfer of the i-TOPCon technology from laboratory into an 8-year-old mc-Si solar cells factory does not only demonstrate the high efficiency of TOPCon technology but also the feasibility for upgrading existing old cell factories, which is meaningful to the silicon wafer-based PV industry.

## ACKNOWLEDGEMENTS

The authors would like to thank the National 10,000 Talents Program in China and the Technology Top Runner Program of China.

## ORCID

Yifeng Chen  <https://orcid.org/0000-0001-8601-0979>

## REFERENCES

- Chen Y, Altermatt PP, Chen D, et al. From laboratory to production: learning models of efficiency and manufacturing cost of industrial crystalline silicon and thin film photovoltaic technologies. *IEEE J Photovoltaics*. 2018;8(6):1531-1538.
- Blakers AW, Wang A, Milne AM, Zhao J, Green MA. 22.8% efficient silicon solar cell. *Appl Phys Lett*. 1989;55(13):1363-1365.
- Altermatt PP, Chen Y, Yang Y, Feng Z. Riding the workhorse of the industry: PERC. *Photovolt Int*. 2018;41:46-54.
- Rüdiger M, Steinkemper H, Hermle M, Glunz SW. Numerical current density loss analysis of industrially relevant crystalline silicon solar cell concepts. *IEEE J Photovoltaics*. 2014;4(2):533-539.
- Altermatt PP, Yang Y, Chen Y, Chen D, Zhang X, Xu G, Feng Z, "Learning from the past to look beyond the roadmap of PERC Si solar cell mass production", 35th EU PV Solar Energy Conf 2018:215-221.
- Schmidt J, Peibst R, Brendel R. Surface passivation of crystalline silicon solar cells: present and future. *Sol Energy Mater Sol Cells*. 2018;187:39-54.
- Melskens J, van de Loo BH, Macco B, Black LE, Smit S, Kessels WMM. Passivating contacts for crystalline silicon solar cells: from concepts and materials to prospects. *IEEE J Photovolt*. 2018;8(2):373-388.
- Taguchi M, Tanaka M, Matsuyama T, Matsuoka T, Tsuda S, Nakano S, Kishi Y, Kuwano Y, "Improvement of the conversion efficiency of polycrystalline silicon thin film solar cell", Tech. Digest of the International PVSEC-5 Conference. Kyoto, Japan; 1990: 689-692.
- Masuko K, Shigematsu M, Hashiguchi T, et al. Achievement of more than 25% conversion efficiency with crystalline silicon heterojunction solar cell. *IEEE J Photovoltaics*. 2014;4(6):1433-1435.
- Adachi D, Hernández JL, Yamamoto K. Impact of carrier recombination on fill factor for large area heterojunction crystalline silicon solar cell with 25.1% efficiency. *Appl Phys Lett*. 2015;107(23):233506.
- Yoshikawa K, Kawasaki H, Yoshida W, et al. Silicon heterojunction solar cell with interdigitated back contacts for a photoconversion efficiency over 26%. *Nat Energy*. 2017;2(5):17032.
- Takagi M, Nakayama K, Terada C, Kamioka H. Improvement of the shallow base transistor technology by using a doped polysilicon diffusion source. *J Jap Soc Appl Phys (Suppl)*. 1972;42:101.
- Grad J, Glasl A, Murrmann H. High-performance transistors with arsenic-implanted polysil emitters. *IEEE J Solid-State Circuits*. 1976; SC-11:491.
- Seto JYW. The electrical properties of polycrystalline silicon films. *J Appl Phys*. 1975;46(12):5247-5254.
- Matsushita T, Aoki T, Otsu T, et al. Semi-insulating polycrystalline-silicon (SIPOS) passivation technology. *J Jap Appl Phys (Suppl)*. 1976;15(S1):35.
- Mochizuki H, Aoki T, Yamoto H, Okayama M, Abe M, Ando T. Semi-insulating polycrystalline-silicon (SIPOS) films applied to MOS integrated circuits. *Jpn J Appl Phys*. 1976;15(S1):41.
- De Graff HC, de Groat JG. The SIS tunnel emitter: a theory for emitters with thin interface layers. *IEEE Trans Electron Devices*. 1979;ED-26(11):1771.
- Swanson RM, "Thermophotovoltaic solar energy conversion", Materials Research at Stanford University Annual Report;1979:369.
- Green MA, Blakers AW. Advantages of metal-insulator semiconductor structures for silicon solar cells. *Sol Cells*. 1983;8(1):3-16.
- Yablonovitch E, Gmitter T, Swanson RM, Kwark YH. A 720 mV open circuit voltage SiO<sub>x</sub>:c-Si: SiO<sub>x</sub> double heterostructure solar cell. *Appl Phys Lett*. 1985;47(11):1211-1213.
- Tarr NG. A polysilicon emitter solar cell. *IEEE Electron Dev Lett*. 1985;6(12):655-658.
- Gan JY, Swanson RM, "Polysilicon emitters for silicon concentrator solar cells", in: Proceedings 21st IEEE Photovolt. Spec. Conference. IEEE, Kissimmee, Florida;1990: 245-250.
- Cousins PJ, Smith DD, Luan H, Manning J, Dennis TD, Waldhauer A, Wilson KE, Harley G., Mulligan WP, "Generation 3: improved performance at lower cost", 35th IEEE PV Specialists Conf. Honolulu;2010;71.
- Feldmann F, Bivour M, Reichel C, Hermle M, Glunz SW. Passivated rear contacts for high-efficiency n-type Si solar cells providing high interface passivation quality and excellent transport characteristics. *Sol Energy Mater Sol Cells*. 2014;120:270-274.
- Glunz SW, Feldmann F. SiO<sub>2</sub> surface passivation layers—a key technology for silicon solar cells. *Sol Energy Mater Sol Cells*. 2018;185:260-269.
- Richter A, Benick J, Feldmann F, Fell A, Hermle M, Glunz SW. n-Type Si solar cells with passivating electron contact: identifying sources for efficiency limitations by wafer thickness and resistivity variation. *Sol Energy Mater Sol Cells*. 2017;173:96-105.
- Haase F, Hollemann C, Schäfer S, et al. Laser contact openings for local poly-Si-metal contacts enabling 26.1% efficient POLO-IBC solar cells. *Sol Energy Mater Sol Cells*. 2018;186:184-193.
- Chen Y, Chen D, Liu C, Wang Z, Yang Z, He Y, Xu G, Zhang X, Yang Y, Altermatt PP, Feng Z, Verlinden P, "The path to 25% large-area industrial crystalline silicon solar cells", 3rd N-type c-Si Cell and Passivated Contact Forum. Changzhou, China; 2018.
- Kane DE, Swanson RM, "Measurement of the emitter saturation current by a contactless photo conductivity decay method", in: Proceedings of the 18<sup>th</sup> IEEE Photovoltaic Specialists Conference. 1985;578-583.
- Liu B, Chen Y, Yang Y, et al. Improved evaluation of saturation currents and bulk lifetime in industrial Si solar cells by the quasi steady state photo conductance decay method. *Sol Energy Mater Sol Cells*. 2016;149:258-265.
- Rienäcker M, Bossmeyer M, Merkle A, et al. Junction resistivity of carrier-selective polysilicon on oxide junctions and its impact on solar cell performance. *IEEE J Photovolt*. 2017;7(1):11-18.

32. Herasimenka SY, Dauksher WJ, Bowden SG. >750 mV open circuit voltage measured on 50  $\mu\text{m}$  thick silicon heterojunction solar cell. *Appl Phys Lett*. 2013;103(5):053511.
33. Green MA. Solar cell fill factors: general graph and empirical expressions. *Solid-State Electron*. 1981;24(8):788-789.
34. Veith-Wolf BA, Schäfer S, Brendel R, Schmidt J. Reassessment of intrinsic lifetime limit in n-type crystalline silicon and implication on maximum solar cell efficiency. *Sol Energy Mater Sol Cells*. 2018;186:194-199.
35. Richter A, Werner F, Cuevas A, Schmidt J, Glunz SW. Improved parameterization of Auger recombination in silicon. *Energy Procedia*. 2012;27:88-94.
36. <https://www.imec-int.com/en/articles/imec-and-jolywood-achieve-a-record-of-23-2-percent-with-bifacial-n-pert-solar-cells>

**How to cite this article:** Chen Y, Chen D, Liu C, et al. Mass production of industrial tunnel oxide passivated contacts (i-TOPCon) silicon solar cells with average efficiency over 23% and modules over 345 W. *Prog Photovolt Res Appl*. 2019;27:827-834. <https://doi.org/10.1002/ppp.3180>